Title

In cellulo phosphorylation induces pharmacological reprogramming of maurocalcin, a cell-penetrating venom peptide

Journal

Proceedings of the National Academy of Sciences of the United States of America, 113(17)

ISSN

0027-8424

Authors

Ronjat, Michel
Feng, Wei
Dardevet, Lucie
et al.

Publication Date

2016-04-26

DOI

10.1073/pnas.1517342113

Peer reviewed

In cellulo phosphorylation induces pharmacological reprogramming of maurocalcin, a cell-penetrating venom peptide

Michel Ronjat[a,b,1,2], Wei Feng[c,1], Lucie Dardevet[a,b], Yao Dong[c], Sawsan Al Khoury[a,b], Franck C. Chatelain[d,e], Virginie Vialla[a,b,f], Samir Chahboun[a,b], Florian Lesage[d,e], Hervé Darbon[g], Isaac N. Pessah[c], and Michel De Waard[a,b,f,2]

[a]INSERM U836, LabEx Ion Channel, Science and Therapeutics, Grenoble Institute of Neuroscience, 38042 Grenoble, France; [b]Université Grenoble Alpes, 38042 Grenoble, France; [c]Department of Molecular Biosciences, School of Veterinary Medicine, University of California, Davis, CA 95616; [d]CNRS UMR 7275, LabEx Ion Channel, Science and Therapeutics, Institut de Pharmacologie Moléculaire et Cellulaire, F-06560 Valbonne, France; [e]Université de Nice Sophia Antipolis, F-06560 Nice, France; [f]Smartox Biotechnologies, 38400 Saint-Martin d'Hères, France; and [g]Architecture et Fonction des Macromolécules Biologiques-CNRS UMR 7257, Aix-Marseille Université, 13009 Marseille, France

Edited by Andrew R. Marks, Columbia University College of Physicians & Surgeons, New York, NY, and approved February 25, 2016 (received for review August 31, 2015)

The venom peptide maurocalcin (MCa) is atypical among toxins because of its ability to rapidly translocate into cells and potently activate the intracellular calcium channel type 1 ryanodine receptor (RyR1). Therefore, MCa is potentially subjected to posttranslational modifications within recipient cells. Here, we report that MCa Thr^{26} belongs to a consensus PKA phosphorylation site and can be phosphorylated by PKA both in vitro and after cell penetration in cellulo. Unexpectedly, phosphorylation converts MCa from positive to negative RyR1 allosteric modulator. Thr^{26} phosphorylation leads to charge neutralization of Arg^{24}, a residue crucial for MCa agonist activity. The functional effect of Thr^{26} phosphorylation is partially mimicked by aspartyl mutation. This represents the first case, to our knowledge, of both ex situ posttranslational modification and pharmacological reprogramming of a small natural cystine-rich peptide by target cells. So far, phosphorylated MCa is the first specific negative allosteric modulator of RyR1, to our knowledge, and represents a lead compound for further development of phosphatase-resistant analogs.

maurocalcin | phosphorylation | pharmacology | toxin | ryanodine receptor

Animal venoms represent biolibraries that are natural sources for the discovery of a growing number of peptides with important pharmacological properties. These peptides have been instrumental in discriminating different subtypes of ion channels and membrane receptors (1–3). Several of them are now approved by the US Food and Administration for the treatment of various human pathological conditions (4). Maurocalcin (MCa) is a 33-amino acid peptide that belongs to the family of the calcin toxins characterized by their folding forming an inhibitor cystine knot motif (5, 6). After its initial purification from the venom of the scorpion *Scorpio maurus palmatus*, MCa was obtained as a synthetic peptide that exhibits structural and pharmacological properties identical to those of the natural peptide (7). Extensive characterization of MCa identified it as one of the most potent effectors of ryanodine receptor type 1 (RyR1) (8, 9). RyR1 is one of the three isoforms that make up the RyR intracellular calcium channels family. It was first identified in skeletal muscles (10) but is also broadly expressed in many other tissues such as pre- and postsynaptic sites within neurons of the brain (11). RyR calcium channels regulate Ca^{2+} release from intracellular stores, and therefore represent crucial players of a number of physiological and toxicological processes, from muscle contraction to gene expression (12). As a consequence, silencing of the gene encoding RyR1 is lethal at birth (13). Despite extensive studies of the RyR biophysical properties, only a few molecules specifically acting on these calcium channels have been identified. The only specific inhibitors of RyR1 known so far are ryanodine at high concentration (14), although this compound also exhibits agonist properties at low doses (15, 16), and dantrolene. Ruthenium red lacks selectivity and cell permeability. On the agonist side, MCa is a very informative pharmacologic tool to investigate RyR properties because of its nanomolar potency and novel ability to stabilize long-lived subconductances of the channel. Accordingly, MCa increases specific binding of [^{3}H]-ryanodine to RyR1 with an apparent affinity in the range of 10 to 50 nM (9). This effect results from the ability of MCa to convert RyR1 low-affinity ryanodine binding sites into high-affinity sites, increase RyR1 sensitivity to activating low Ca^{2+} concentrations (μM), and decrease RyR1 sensitivity to inhibiting high Ca^{2+} concentrations (mM), with the two latest effects probably requiring an allosteric mechanism. MCa binding onto RyR1 also induces Ca^{2+} release from sarcoplasmic reticulum vesicles (8). These effects correlate with the induction by MCa of long-lasting subconductance open transitions of purified RyR1 channels reconstituted in artificial lipid bilayers (7, 17, 18). This positive allosteric activity of MCa is the consequence of its interaction with a cytoplasmic RyR1 domain that directly controls the gating of this calcium channel (19). Production of MCa analogs after alanine scanning helped identifying critical residues involved in the positive allosteric activity of the peptide (9, 20). The pharmacophore of MCa was restricted to a few basic amino acid residues, among which Arg^{24}

Significance

Animal toxin peptides typically exhibit high affinity and selectivity for specific subclasses of cell receptors that account for their activity. Posttranslational modifications of toxin sequences may occur in the venom gland machinery, but there is no example so far of toxins being subjected to such modifications ex situ after delivery to target cells. Here, we provide evidence that the cell permeant maurocalcin (MCa), found in scorpion venom, undergoes PKA-mediated phosphorylation in cellulo, and that posttranslational modification leads to its complete pharmacological reprogramming activity toward ryanodine receptor type 1 (RyR1), a key player in Ca^{2+} homeostasis in excitable cells. Phosphorylation converts MCa from a potent stabilizer of RyR1 channel substates to a negative allosteric modulator that mitigates RyR1 channel Ca^{2+} leak.

Author contributions: M.R., I.N.P., and M.D.W. designed research; M.R., W.F., Y.D., S.A.K., V.V., S.C., H.D., and I.N.P. performed research; M.R., W.F., L.D., F.C.C., F.L., H.D., I.N.P., and M.D.W. analyzed data; and M.D.W. wrote the paper.

The authors declare no conflict of interest.

This article is a PNAS Direct Submission.

[1]M.R. and W.F. contributed equally to this work.

[2]To whom correspondence may be addressed. Email: michel.dewaard@univ-nantes.fr or michel.ronjat@ujf-grenoble.fr.

This article contains supporting information online at www.pnas.org/lookup/suppl/doi:10.1073/pnas.1517342113/-/DCSupplemental.

was the most important for activity (9). Despite these extensive studies, none of the mutations converted MCa into RyR1 antagonist peptide, but mostly lowered affinity or inhibited agonist effect.

It is highly unusual that a venom peptide targets an intracellular receptor. Several reports indicate that MCa binds cell surface glycosaminoglycans (21) and membrane lipids (20), and that it rapidly translocates into cells using mechanisms akin to cell-penetrating peptides (CPPs) (22). As a matter of fact, MCa and CPPs share interesting structural features, such as the presence of a strong dipole moment characterized by a heavily basic face opposing a far less charged one (23–25), with the latter being also quite hydrophobic. Similar to a CPP, MCa proved to be efficient in the transport of several types of cargoes ranging from drugs to peptides, proteins, and nanoparticles (22, 26–32). MCa is the first natural CPP, to our knowledge, emerging from venom sources and whose cytoplasm delivery and activity could be straightforwardly examined through the activation of RyR channels (33). It is therefore conceivable that MCa may undergo posttranslational modifications by target cell enzymes on delivery into the cytoplasm.

In this report, we show that MCa is a substrate of PKA in vitro, leading to the phosphorylation of Thr^{26}. We also demonstrate that MCa phosphorylation happens in cellulo after translocation. Phosphorylation of MCa leads to a fine peptide structural modification responsible for its complete pharmacological reprogramming, thereby converting MCa into a RyR1 antagonist. We thus establish for the first time, to our knowledge, that the pharmacological properties of a small cell-penetrating toxin peptide can be dramatically modified by posttranslational modification, opening

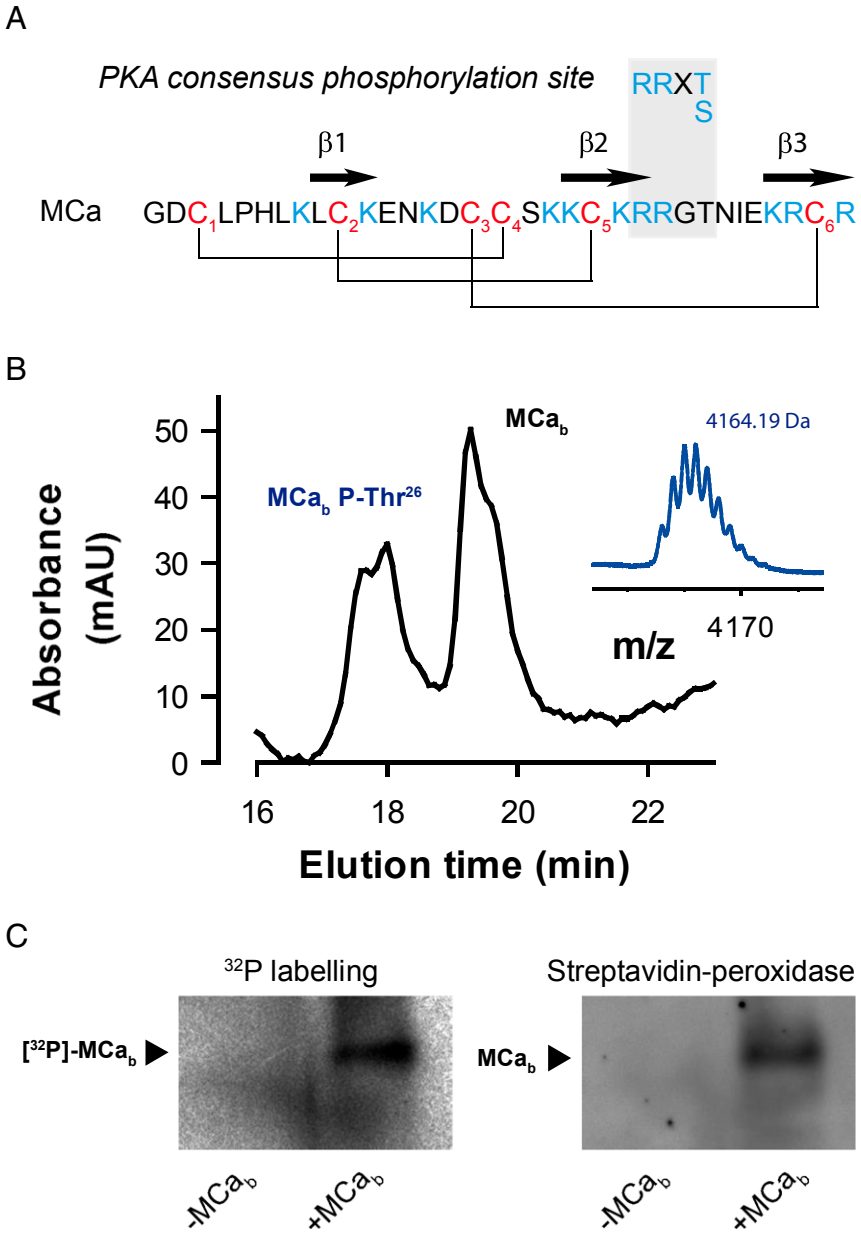

Fig. 1. MCa is phosphorylated by PKA. (*A*) Identification of a consensus phosphorylation site in MCa primary structure. (*B*) In vitro phosphorylation of MCa_b by the catalytic subunit of PKA. Shift in the HPLC profile of MCa_b induced by phosphorylation by PKA. (*Inset*) Mass spectrometry profile illustrating the appearance of the phosphorylated MCa_b variant. Representative of $n = 3$. (*C*) In cellulo phosphorylation of MCa_b. HEK293 cells were incubated with [^{32}P]-orthophosphoric acid in the presence or absence of MCa_b. (*Left*) Autoradiogram showing the appearance of [^{32}P]-MCa_b. (*Right*) Labeling of MCa_b with streptavidin-peroxidase. Representative of $n = 2$.

innovative approaches to develop negative allosteric modulators of the RyR1 channel, with MCa P-Thr^{26} as a promising lead.

Results

MCa Is Phosphorylated by Protein Kinase A. Analysis of MCa sequence reveals a consensus R-R-X-T site of phosphorylation by PKA at position R^{23}R^{24}G^{25}T^{26}, indicating that Thr^{26} may get phosphorylated (Fig. 1*A*). This phosphorylation site is conserved throughout the members of the calcin toxin family that include imperatoxin A (34), hemicalcin (35), opicalcin 1 (6), and hadrucalcin (36), indicating that phosphorylation may be a common feature of these toxins acting as RyR1 agonists. Opicalcin 2 is the only toxin of this family that lacks this consensus sequence (6). According to the 3D structure of MCa (23) and earlier alanine scan studies (9, 18, 20), the domain encompassing R^{23}R^{24}G^{25}T^{26} lays in the pharmacophore region of the peptide, making this site both accessible to PKA phosphorylation (23) and of potential functional importance (*SI Appendix*, Fig. S1*A*). We first investigated in vitro MCa phosphorylation by the catalytic subunit of PKA. Phosphorylation was assessed by analytical HPLC and mass spectrometry (MS) (*SI Appendix*, Fig. S1*B*). As shown, phosphorylation induces a leftward shift in the HPLC profile of MCa$_b$ (N-terminal biotinylated version of MCa) indicative of reduced peptide hydrophobicity. MS spectra recording by MALDI-TOF of the resulting product shows the appearance of an experimental molecular mass of $(M+H^+)^+$ 4,164.19 Da (Fig. 1*B*, inset) corresponding to the expected theoretical molecular mass of phosphorylated MCa$_b$ (MCa$_b$ P-Thr^{26} at 4,164.20 Da), in addition to the mass of the unphosphorylated one [$(M+H^+)^+$ at 4,084.70 Da]. To confirm that phosphorylation takes place at Thr^{26} residue, the mutated MCa$_b$ Thr^{26}Glu analog was used as negative control in the phosphorylation experiment. Both HPLC and MS analyses failed to detect the appearance of phosphorylated MCa$_b$ Thr^{26}Glu (*SI Appendix*, Fig. S1*B*). These data indicate that Ser^{18}, the only other residue that could experimentally undergo phosphorylation in MCa sequence, is not targeted by PKA. Examination of MALDI-TOF spectra of crude *Maurus palmatus* venom, from which MCa was originally discovered, failed to uncover a mass corresponding to phosphorylated MCa. Thus, we investigated whether MCa could be phosphorylated after cell penetration into the cytoplasm of target cells. After 3 h of incubation of HEK293 cells with MCa$_b$ in the presence of [^{32}P]-orthophosphoric acid, cytoplasmic MCa$_b$ was isolated and phosphorylation witnessed by autoradiography. As shown, a ^{32}P-labeled band appeared in cells incubated with MCa$_b$, but not in the absence of MCa$_b$ (Fig. 1*C*). The identification of this band was confirmed by streptavidin-peroxidase labeling. These data therefore constitute evidence that MCa phosphorylation can occur ex situ and in cellulo after cell penetration into recipient cells.

Interaction of MCa with RyR1 Is Preserved After Phosphorylation. To produce a fully phosphorylated MCa$_b$, the chemical synthesis of MCa$_b$ P-Thr^{26} was performed [*SI Appendix*, Fig. S2 (37)]. Binding of purified RyR1 on variable concentrations of MCa$_b$ or P-MCa$_b$ Thr^{26} was measured using streptavidin-covered beads. Bound RyR1 was then measured by immune staining, using antibody directed against RyR1 (38). As shown, the amount of bound RyR1 increases with the concentration of MCa$_b$ or P-MCa$_b$ Thr^{26}, reaching plateau at 100 nM for MCa$_b$ and 300 nM for P-MCa$_b$ Thr^{26} (Fig. 2*A*). Apparent affinities of RyR1 are 58.2 nM for MCa$_b$ and 149.6 nM for P-MCa$_b$ Thr^{26} (Fig. 2*B*). Binding of RyR1 on MCa$_b$ P-Thr^{26} is strongly inhibited by an excess of nonbiotinylated MCa (Fig. 2*C*), indicating that MCa precludes phosphorylated MCa binding on RyR1.

MCa Pharmacological Reprogramming by Phosphorylation. MCa is a strong positive allosteric modulator of RyR1, and channel openings have been associated with a pronounced enhancement of [^{3}H]-ryanodine binding (7–9, 18, 20, 39). In sharp contrast to

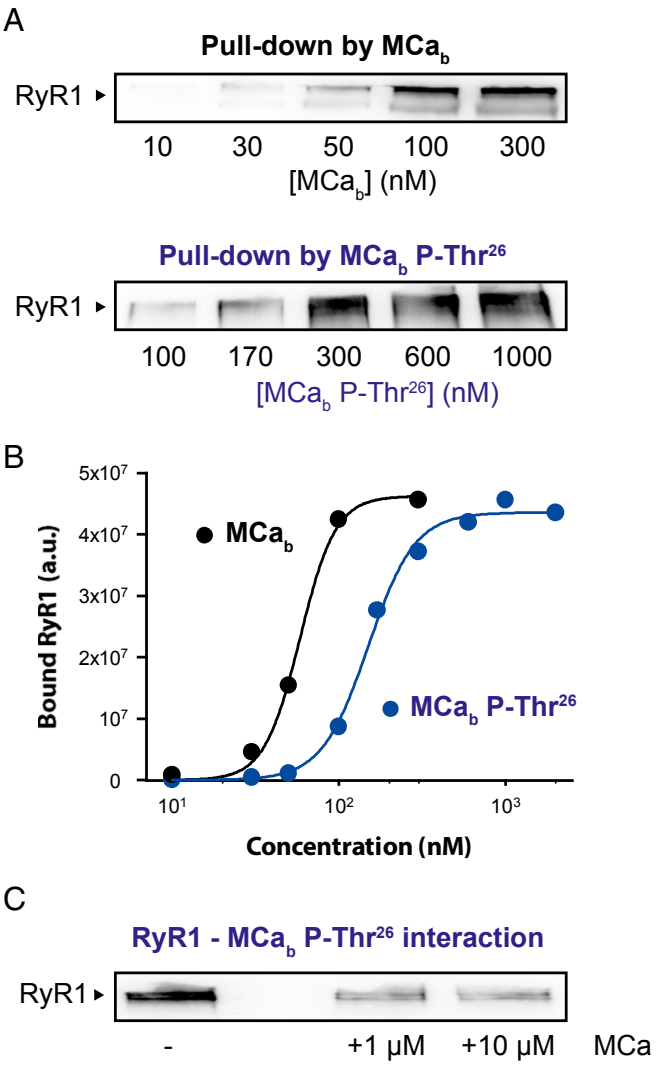

Fig. 2. Direct interaction of MCa$_b$ P-Thr^{26} with purified RyR1. (*A*) Western blot analyses of RyR1 on interaction with variable concentrations of MCa$_b$ or MCa$_b$ P-Thr^{26} immobilized on streptavidin-covered beads. (*B*) Concentration dependence of RyR1 pull-down by MCa$_b$ or MCa$_b$ P-Thr^{26}. Data were fitted by Hill-type sigmoid functions of the type $y = (a.x^b)/(c^b + x^b)$, where $a = 4.6 \times 10^7 \pm 0.2 \times 10^7$ a.u. (MCa$_b$) and $4.4 \times 10^7 \pm 0.1 \times 10^7$ a.u. (MCa$_b$ P-Thr^{26}), $b = 4.0 \pm 0.6$ (MCa$_b$) and 3.1 ± 0.3 (MCa$_b$ P-Thr^{26}), and $c = 58.2 \pm 2.6$ nM (MCa$_b$) and 149.7 ± 5.8 nM (MCa$_b$ P-Thr^{26}). a.u. = arbitrary unit. (*C*) Western blot of RyR1 showing extent of pull-down by 170 nM MCa$_b$ P-Thr^{26}/streptavidin-coated beads in the absence and presence of an excess nonbiotinylated 1 μM MCa. Representative of $n = 2$.

the reported effects of MCa, 5–10 μM MCa$_b$ P-Thr^{26} was found to inhibit the binding of [^{3}H]-ryanodine onto RyR1, provided we used 1 nM [^{3}H]-ryanodine and assessed binding for 30 min (Fig. 3*A*). Use of higher concentrations of [^{3}H]-ryanodine and longer incubation times led to the loss of this inhibition ($n = 4$). These data indicate that MCa phosphorylation onto Thr^{26} precludes the agonist effect and favors inhibition.

Next, the effect of MCa$_b$ P-Thr^{26} was investigated on Ca^{2+} release from Ca^{2+}-loaded sarcoplasmic reticulum (SR) vesicles. As expected from earlier reports (8, 9), 50 nM MCa$_b$ induces a strong Ca^{2+} release from Ca^{2+}-loaded SR vesicles despite the maintained activity of the SR ATPase Ca^{2+} pump (Fig. 3*B*). In contrast, a 20-fold higher concentration of MCa$_b$ P-Thr^{26} (1 μM) is unable to promote net Ca^{2+} release from SR vesicles, whereas a subsequent addition of 100 nM MCa$_b$ still induces a strong

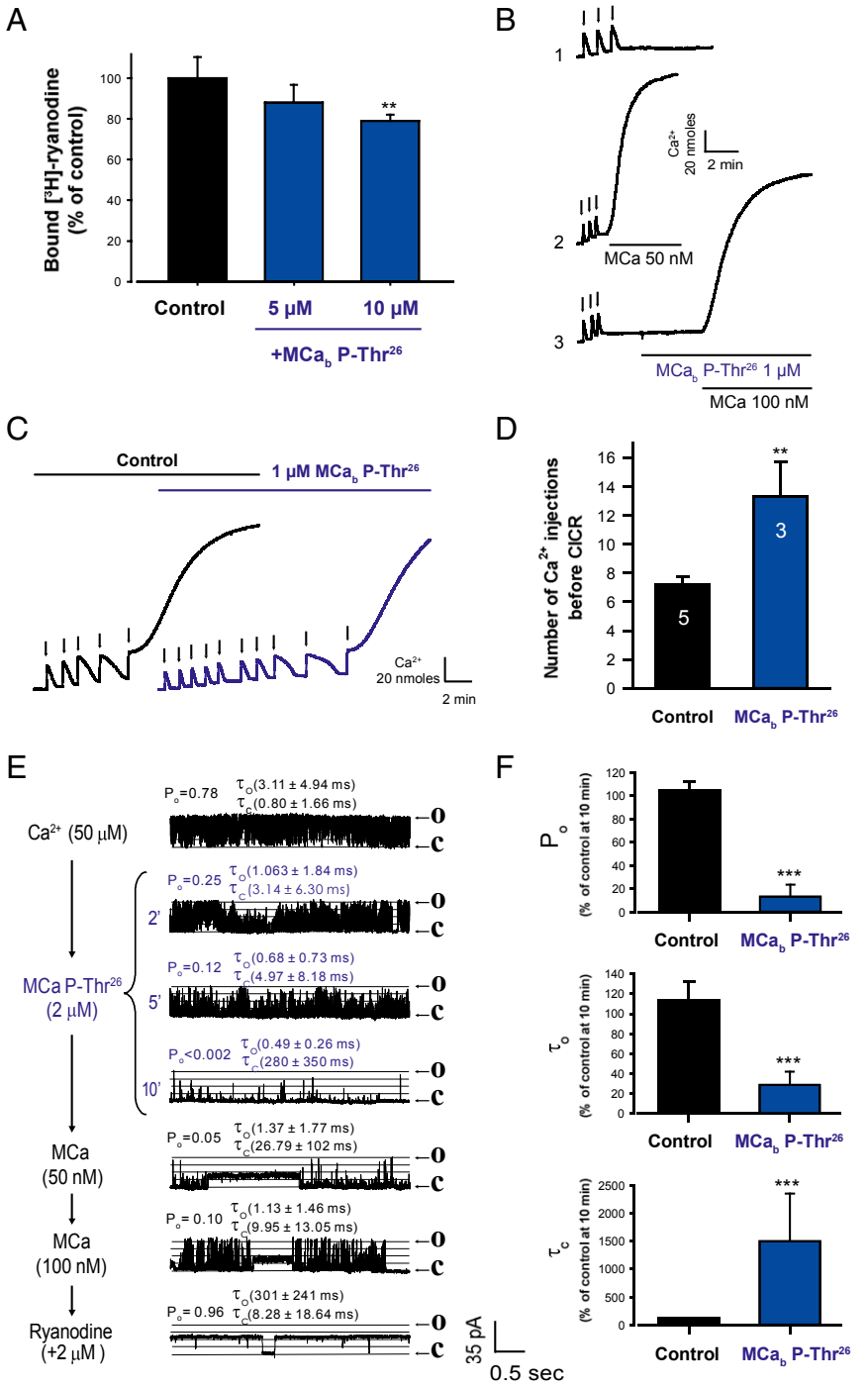

Fig. 3. Phosphorylation confers RyR1 antagonistic properties to MCa_b. (*A*) MCa_b P-Thr^{26} produces a mild reduction in [^{3}H]-ryanodine binding onto SR vesicles. SR, 100 μg/mL, pCa 5, SR pretreated at 25 °C with MCa_b P-Thr^{26} before a 30-min incubation at 37 °C with 1 nM [^{3}H]-ryanodine (mean ± SD, $n = 5$). (*B*) MCa_b P-Thr^{26} does not induce Ca^{2+} release from SR vesicles. (1) Control experiments showing SR vesicle Ca^{2+} loading by three successive additions of 20 nmol Ca^{2+} (arrows). (2) Ca^{2+} release induced by 50 nM MCa after SR loading with three identical additions of Ca^{2+}. (3) Addition of MCa_b P-Thr^{26} (1 μM) to Ca^{2+}-loaded SR vesicles does not induce Ca^{2+} release. Subsequent addition of 100 nM MCa efficiently releases Ca^{2+}. (*C*) Inhibition of Ca^{2+}-induced Ca^{2+} release by 1 μM MCa_b P-Thr^{26}. The presence of MCa_b P-Thr^{26} doubles the number of Ca^{2+} additions required for CICR. (*D*) Number of Ca^{2+} injections required to trigger CICR in the presence of 1 μM MCa_b P-Thr^{26} ($n = 8$ experiments). (*E*) MCa_b P-Thr^{26} (2 μM) causes a time-dependent inhibition of RyR1 channel activity (traces 2–4) that can be reactivated by MCa. Sequential additions of ligands into the *cis* solution were denoted with downward arrows on the left side of each representative current trace. Open probability (P_o), mean open- and closed-dwelling time constants obtained for each recording condition were denoted above each representative trace. "O" and "C" in the figure indicate the full and zero conductance states when the channel fully opened and closed, respectively. Total $n = 7$ independent bilayer measurements under similar conditions produced consistent responses. (*F*) RyR1 gating parameters (Po, τ_o, and τ_c) in the absence and presence of MCa_b P-Thr^{26} (at 10 min after application) as percentage of control condition. Data are presented by mean ± SD; control group (vehicle), $n = 3$; group with MCa_b P-Thr^{26}, $n = 4$. $^{**}P < 0.005$; $^{***}P < 0.001$.

release of Ca^{2+}, indicating the functionality of the SR vesicles (Fig. 3*B*). MCa_b P-Thr^{26} does not act as a weak agonist by producing a partial depletion from SR vesicles. Indeed, the slope of Ca^{2+} release from SR vesicles after loading was negative, on

average, in the presence of 1 μM MCa_b P-Thr^{26} (*SI Appendix*, Fig. S3*A*), and the total Ca^{2+} content in SR vesicles remained identical to the nontreated SR vesicles, as assessed by Ca^{2+} release, triggered by the application of 1 μM of the A23187 Ca^{2+} ionophore (*SI Appendix*, Fig. S3 *B* and *C*). These results indicate that MCa should have the ability to displace MCa_b P-Thr^{26} from its binding site on RyR1. Similarly, the agonists caffeine (2 mM) and ryanodine (20 μM) were also found to keep their Ca^{2+} release-activating effects in the presence of 2 μM MCa_b P-Thr^{26} (*SI Appendix*, Fig. S4 *A* and *B*). A more physiological process of RyR1 activation is the process of calcium-induced calcium release (CICR), whereby cytoplasmic Ca^{2+} triggers RyR1 opening and Ca^{2+} release from SR (40). Sensitivity of SR vesicles to CICR can be measured by sequential addition of Ca^{2+} to the SR vesicle medium that will lead to CICR (41). Under control conditions, SR vesicle loading by seven additions of Ca^{2+} (280 nmol) is required to trigger CICR, whereas induction of CICR requires up to 13 additions of Ca^{2+} (520 nmol) in the presence of 1 μM MCa_b P-Thr^{26} (Fig. 3 *C* and *D*). This result indicates that MCa_b P-Thr^{26} attenuates the response of RyR1 to cytoplasmic activating Ca^{2+}.

To more directly explore the inhibitory effect of MCa_b P-Thr^{26}, we measured single-channel gating activity of RyR1 reconstituted in bilayer lipid membranes. In the presence of optimal cytosolic (*cis*) Ca^{2+} concentration (50 μM), typical RyR1 channels exhibit a high open probability (P_o) of 0.78 with characteristic, very short-lived transitions to the full open state (Fig. 3*E*). The addition of 2 μM MCa_b P-Thr^{26} into the *cis* chamber produced a very strong channel gating inhibition in a time-dependent manner (Fig. 3*E*). This time-dependent reduction in P_o was invariably observed ($n = 7$ channels) and suggests that multiple sites on RyR1 may need to be occupied to see full inhibition. Kinetic analysis of RyR1 gating indicates a ∼fourfold decrease in mean open dwell time and a ∼13-fold increase in mean closed dwell time, resulting in an eightfold decrease in P_o 10 min after addition of MCa_b P-Thr^{26} (Fig. 3*F*). Subsequent addition of 50 nM MCa into the *cis* chamber resulted in reactivation of RyR1, as witnessed by the appearance of the MCa-induced characteristic (7–9, 17, 18) long-lasting subconductance states (Fig. 3*E*). Moreover, MCa-modified RyR1 channel remains responsive to 2 μM ryanodine, as witnessed by the appearance of a different long-lasting subconductance state (Fig. 3*E*). In addition to MCa and ryanodine, RyR1 channels inhibited by 3 μM MCa_b P-Thr^{26} could also be reactivated by the addition of 2 mM caffeine to the *cis* chamber. In turn, these caffeine-reactivated channels remained responsive to 50 nM MCa (*SI Appendix*, Fig. S5*A*). Altogether, evidence of reactivation of channel activity by the RyR1 agonists MCa, ryanodine, and caffeine further illustrate the fact that MCa, as well as ryanodine or caffeine, overcome the effect of MCa_b P-Thr^{26} on RyR1, explaining why the inhibition of [^{3}H]-ryanodine binding by MCa_b P-Thr^{26} is difficult to observe. This overriding effect of caffeine on P_o suppression by MCa_b Thr^{26} probably occurs through an allosteric mechanism, considering that caffeine and calcins bind onto distinct sites. Finally, we also determined that application of 2 μM MCa_b P-Thr^{26} lowers the channel P_o without promoting the subconductance state of RyR1, indicating again that this analog is not a weak activator (*SI Appendix*, Fig. S5*B*). Altogether, these results lead to the hypothesis that MCa_b P-Thr^{26} decreases RyR1 sensitivity to activating Ca^{2+} concentrations; hence the term negative allosteric modulator for MCa_b P-Thr^{26}.

Thr^{26} Phosphorylation Leads to Neutralization of the Guanidinium Group of Arg^{24}. Preserving the 3D structure of MCa is mandatory for its pharmacological activity (42). Although a pharmacophore has been mapped that is responsible for the agonist activity of MCa (9, 20, 24), none of the analogs previously produced exhibit inhibitory activity. The consequences of Thr^{26} phosphorylation on MCa structure were thus expected to be subtle, and were therefore fully inspected using circular dichroism, ^{1}H-NMR, molecular modeling, and ^{1}H-2D-NMR. Nuclear Overhauser effects in the amide region of MCa and MCa P-Thr^{26} are identical in intensity, showing that the backbone conformation was not altered by the phosphorylation. Both circular dichroism spectra of MCa_b and MCa_b P-Thr^{26} were identical, indicating the preservation of the β-strands (Fig. 4*A*). However, the chemical shifts of several NH protons from backbone and side chains were altered in the region of the pharmacophore (Fig. 4*B*; *SI Appendix*, Fig. S6*A*). These chemical shift variations can be explained by alterations in the chemical environment of the atomic nuclei located in the immediate vicinity of the phosphate group now present onto the hydroxyl moiety of Thr^{26} (43). Protons of amino acid residues 20–23 and 30–33 of MCa_b P-Thr^{26}, close to the phosphoryl group, are indeed expected to shift orientation relative to the peptide backbone (23). A total of 25 3D projections of MCa_b P-Thr^{26} were modeled, using the 25 deposited structures of MCa (Protein Data Bank ID code 1C6W). Twelve of the modeled 3D structures were found to be in agreement with the ^{1}H-NMR data acquired on MCa_b P-Thr^{26} and predicted a reorientation of the lateral chain of Arg^{24} and an electrostatic interaction with the lateral chain of the phosphorylated Thr^{26}. Three of 25 modeled structures indicated a possible hydrogen bond interaction of the phosphate group of Thr^{26} with the amine group of Asn^{27}, but were not compatible with the NMR data. To visualize the structural modifications, the average 3D structure of MCa_b P-Thr^{26} (on the basis of the 12 NMR-coherent structures) is superimposed to the corresponding average MCa structure (*SI Appendix*, Fig. S6*B*). As illustrated, the predicted structural changes are observed for amino acid residues 22–33. Nevertheless, the main observation is that the phosphate group on Thr^{26} induces a strong downfield chemical shift variation of the NHε proton of the Arg^{24} side chain (Fig. 4 *B* and *C*). This chemical shift is far more pronounced than the one observed for the NHδ proton of Asn^{27}, indicating that the side chain of Arg^{24} was more likely to move than the one of Asn^{27} in response to Thr^{26} phosphorylation. To confirm the modeling data, the proximity of the guanidinium group of Arg^{24} with the phosphoryl group of Thr^{26} was experimentally measured by ^{1}H-2D-NMR (*SI Appendix*, Fig. S7). We compared the frequency resonance of Arg^{24} guanidinium NHε proton in MCa_b P-Thr^{26} and compared it with MCa. A clear chemical shift variation of this guanidinium group was observed, indicating the vicinity with the phosphoryl group of Thr^{26}. Such an influence of the phosphoryl group was demonstrated earlier (44). Furthermore, results from these experiments show that the Asn^{27} side chain is negligibly affected by the modification of Thr^{26}, further ruling out its contribution to the pharmacological reprogramming of MCa_b P-Thr^{26}. The modeled structure of MCa_b P-Thr^{26} illustrating the arginine-phosphate electrostatic interaction is shown in Fig. 4*D*. This type of interaction has been described to present "covalent-like" stability (45), although geometry and distance should affect the stability of this interaction. The resulting structure is in agreement with the reported critical role of Arg^{24} in MCa activity (9). A functional role of Asn^{27} in the pharmacological activity of MCa_b P-Thr^{26}, through the formation of a hydrogen bond between the phosphate group of Thr^{26} and the amine group of Asn^{27} ($n = 3$ of 25 modeled structures) (*SI Appendix*, Fig. S8*A*), was further ruled out by chemically synthesizing and testing two new analogs, MCa_b Asn^{27}Ala and MCa_b P-Thr^{26} Asn^{27}Ala. MCa_b Asn^{27}Ala fully preserves the stimulating activity of MCa on [^{3}H]-ryanodine binding, indicating that Asn^{27} is a priori not a residue of the pharmacophore (*SI Appendix*, Fig. S8*B*). In addition, MCa_b P-Thr^{26} Asn^{27}Ala was found to delay, but not inhibit, caffeine-induced Ca^{2+} release from SR vesicles (*SI Appendix*, Fig. S8*C*). On the basis of these data, we propose that the electrostatic interaction of Thr^{26} phosphate with Arg^{24} guanidinium represents the structural modification of MCa that is involved in its pharmacological reprogramming.

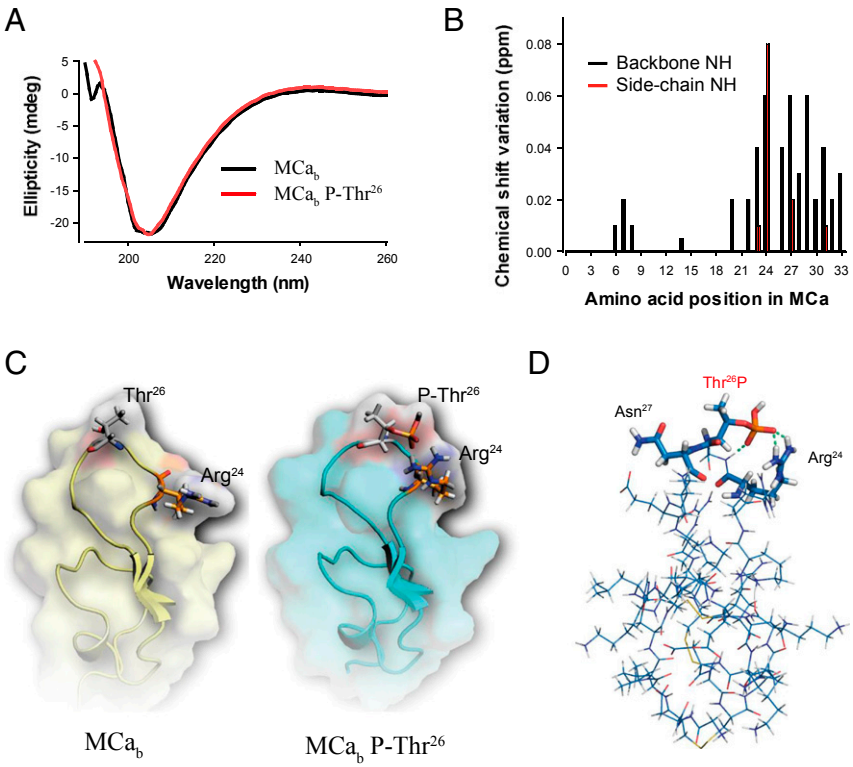

Fig. 4. Structural modifications induced by Thr^{26} phosphorylation. (*A*) Circular dichroism data indicating the conservation of secondary structures of MCa$_b$ after phosphorylation. (*B*) Chemical shift variation (in absolute values) in backbone NH and side-chain NH after Thr^{26} phosphorylation. Note that major variations are observed within the loop encompassing residues 22–31. The structure of MCa P-Thr^{26} was modeled starting with MCa as a structural basis (1C6W from the Protein Database Base). (*C*) 3D structural variations induced by Thr^{26} phosphorylation. MCa structure is in transparency. (*D*) Zoom in on the ionic interaction occurring between the side chains of Thr^{26} and Arg^{24} residues of MCa P-Thr^{26}.

Thr^{26} Substitution by the Negatively Charged Aspartyl Best Mimics Phosphorylation. To test the importance of this intramolecular electrostatic interaction between phosphorylated Thr^{26} and Arg^{24} residues, we chemically synthesized and tested on RyR1 channel activity two closely resembling MCa$_b$ analogs: MCa$_b$ Thr^{26}Glu and MCa$_b$ Thr^{26}Asp. Molecular modeling indicates that the negatively charged carboxylic function of glutamyl is unable to establish an electrostatic interaction with the positively charged guanidinium group of Arg^{24} because of the structural constraints imposed by the rigid backbone of MCa and the superior side-chain length (*SI Appendix*, Fig. S9*A*). The opposite was found to be true for the aspartyl substitution (Fig. 5*A*). This is confirmed by ^{1}H-2D-NMR experiments that indicate a clear chemical shift variation of the Arg^{24} guanidinium NHε proton of MCa$_b$ Thr^{26}Asp compared with MCa, which was not observed for MCa$_b$ Thr^{26}Glu (*SI Appendix*, Fig. S7). These data confirm the importance of peptide backbone geometry for the establishment of salt bridges (46). As shown, 2 μM MCa$_b$ Thr^{26}Asp added into the *cis* chamber produced a time-dependent channel gating inhibition (Fig. 5*B*). However, this inhibition was less pronounced than the one observed with MCa$_b$ P-Thr^{26}. A kinetic analysis of the MCa$_b$ Thr^{26}Asp-modified RyR1 channel indicates a decrease in mean open dwell time (1.9-fold) and an increase in mean closed dwell time (1.6-fold), resulting in a 2.1-fold decrease in P_o 10 min after addition of MCa$_b$ Thr^{26}Asp (Fig. 5*C*). As observed with MCa$_b$ P-Thr^{26}, the MCa$_b$ Thr^{26}Asp-modified RyR1 channel activity remains responsive to the sequential addition of 50 nM MCa and of 2 μM ryanodine (Fig. 5*B*). In contrast, 2 μM MCa$_b$ Thr^{26}Glu increases P_o of RyR1 channels without stabilizing subconductances characteristic of MCa (*SI Appendix*, Fig. S9*B*), and recordings lasting several minutes fail to promote subsequent channel inhibition observed with either MCa$_b$ P-Thr^{26} or MCa$_b$ Thr^{26}Asp. Finally, with regard to Ca^{2+} release from SR, MCa$_b$ Thr^{26}Asp also does not trigger Ca^{2+} release but remains sensitive to 2 mM caffeine or 20 μM ryanodine, akin to MCa$_b$ P-Thr^{26} (*SI Appendix*, Fig. S10). Collectively, these data indicate that Thr^{26} is critical for conferring nanomolar affinity and stabilizing channel subconductance behavior characteristic of MCa. Pharmacological reprogramming of MCa is highly dependent on both the precise electrostatic interaction between MCa$_b$ P-Thr^{26} or its phosphomimic MCa$_b$ Thr^{26}Asp and Arg^{24} and the distance of the negative charge on the Thr^{26} side chain from the ridged MCa backbone (e.g., MCa$_b$ Thr^{26}Asp vs. MCa$_b$ Thr^{26}Glu).

Discussion

Posttranslational modifications such as phosphorylation control the function of a large number of proteins by modifying their ability to interact with their partners and/or by altering their activity (47). Often phosphorylation sites have been found to be located on binding interfaces and to modulate strength of interaction and function (48). Concerning toxins, a number of posttranslational modifications have been reported, all occurring in situ at the site of production within venom glands, and include proteolytic processing, disulphide bridge formation, carboxylation of glutamic acid, bromination of tryptophan, epimerization of some amino acids, cyclization of N-terminal glutamine, and O-glycosylation, to name a few (49). It is of interest that peptides from *Conus* venoms are among the most highly posttranslationally modified gene products (49). In this study, we investigated whether the venom peptide MCa could be phosphorylated ex situ within target cells and examined the consequences of this phosphorylation on its pharmacological properties. MCa presents an interesting combination of features, rarely encountered for peptide toxins, to cross the plasma membrane and to act on an intracellular ion channel target (i.e., RyR1). We report that MCa is a substrate of PKA in vitro and is

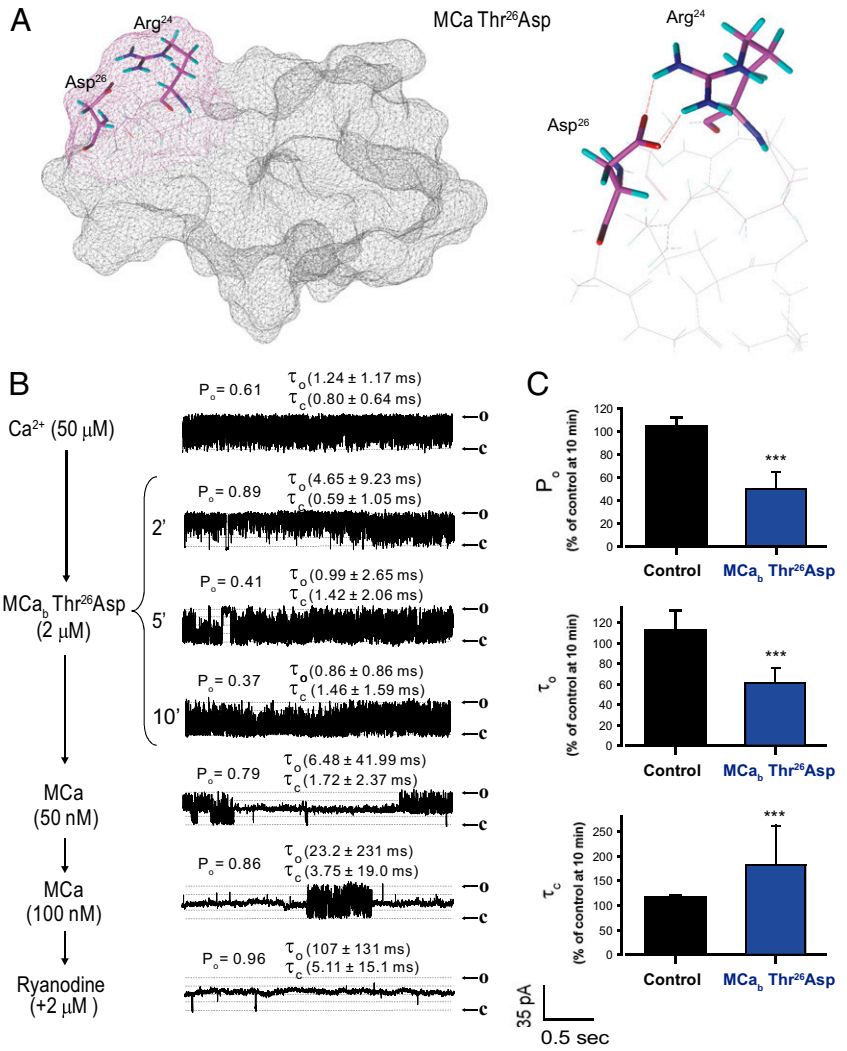

Fig. 5. The MCa_b $Thr^{26}Asp$ partially mimics the antagonist effect of MCa_b P-Thr^{26}. (*A*) 3D structure of MCa $Thr^{26}Asp$ with a zoom in on the ionic interaction occurring between the side chains of Asp^{26} and Arg^{24} residues of MCa $Thr^{26}Asp$ (*Right*). (*B*) MCa_b $Thr^{26}Asp$ (2 μM) causes a time-dependent inhibition of RyR1 channel activity (traces 2–4) that can be reactivated by MCa. Sequential additions of ligands into the *cis* solution were denoted with downward arrows on the left side of each representative current traces. Open probability, mean open- and closed-dwelling time constants (P_o, τ_o, and τ_c) obtained for each recording condition were denoted above each representative trace. "O" and "C" in the figure indicate the full and zero conductance states when the channel fully opened and closed, respectively. Total $n = 11$ independent bilayer measurements under similar conditions produced consistent responses. (*C*) RyR1 gating parameters (P_o, τ_o, and τ_c) in the absence and presence of MCa_b $Thr^{26}Asp$ (at 10 min after application) as a percentage of control condition (control, $n = 3$; MCa_b $Thr^{26}Asp$, $n = 3$).

also phosphorylated in cellulo after cell penetration. To our knowledge, this is the first reported case of an exogenous bioactive peptide that gets phosphorylated within host cells. Probably the most significant discovery is that phosphorylation of MCa provokes its complete pharmacological reprogramming, converting MCa toward an inhibitor of RyR1 activity. Earlier reports about cell phosphorylation of exogenous material concerned clostridial neurotoxins (botulinum neurotoxins A, B, and E and tetanus neurotoxin) (50), but these are very large proteins compared with MCa, and phosphorylation does not negate the activity of these toxins. We provide a clue on how phosphorylation may induce such a drastic change in pharmacological properties of MCa. It is shown here that the negative charge or charges introduced by the phosphate group contribute to both loss of positive allosteric modulation and neutralization of the guanidinium group of Arg^{24}, leading to the conversion toward negative allosteric modulation. The channel bilayer and Ca^{2+} release experiments indicate that MCa_b P-Thr^{26} and MCa_b $Thr^{26}Asp$ reduce channel activity and delay CICR without producing stable subconductances, which is a hallmark of nonphosphorylated MCa, and without fully blocking the channel even at high concentrations. Importantly, the observed MCa_b P-Thr^{26} and MCa_b $Thr^{26}Asp$ effect is the result of forcing the channel to adopt a more "normal" activity, similar to that observed in low cytoplasmic Ca^{2+}, with classical characteristic rapid gating full transitions of RyR1 openings and closings. We thus propose that MCa_b P-Thr^{26} and MCa_b $Thr^{26}Asp$ modify the agonist effect of Ca^{2+} on RyR1; hence the term negative allosteric modulators for these peptides. MCa itself remains a positive allosteric modulator for favoring the activating role of cytoplasmic Ca^{2+} (9). With regard to [^{3}H]-ryanodine binding, we observed a mild inhibition by MCa_b P-Thr^{26} only when performing binding in the presence of low concentrations of [^{3}H]-ryanodine and for a short incubation time. Higher ryanodine concentrations (50 nM) and longer incubation times completely prevented the MCa_b P-Thr^{26} effect. This might be explained by both possible dephosphorylation of MCa_b P-Thr^{26} during the time course of the

experiment with dephosphorylated MCa overriding the effect of MCa_b P-Thr^{26}, and/or ryanodine itself precluding MCa_b P-Thr^{26} effect, as supported by results obtained in bilayer experiments showing the persistence of ryanodine effect on the MCa_b P-Thr^{26}-modified RyR1.

The fact that MCa prevents MCa_b P-Thr^{26} binding on RyR1 suggests their binding occurs on the same site between the clamp and handle domain of RyR1 (51, 52). Although the presence of distinct sites allosterically influencing each other remains possible, it seems, however, unlikely because of the structural similarities between the two ligands being very high and the notion that toxins interact with their receptors through multiple points. However, two binding sites have previously been identified for MCa (19) on RyR1, and therefore the ability of MCa_b P-Thr^{26} to bind to these sites, as well as their respective roles in the effect of MCa_b P-Thr^{26} on RyR1 modulation, remains to be established. In addition, the existence of an allosteric behavior between the MCa and/or MCa_b P-Thr^{26} binding sites within the RyR1 tetramer is also a strong possibility. This could possibly explain the slow onset of action of MCa_b P-Thr^{26}, as well as the rapid overriding effect of MCa on MCa_b P-Thr^{26}. Alternatively, it remains possible that phosphorylation of MCa alters the K_{off} of binding on RyR1 sites, explaining why MCa so easily overrides MCa_b P-Thr^{26}. Interestingly, the reported binding site for imperatoxin A, a close homolog of MCa, is located near the proposed CaM binding site. Knowing that CaM can also act as activator or an inhibitor, depending on Ca^{2+} concentration, there is an interesting parallel to be made on the opposing effects of MCa_b P-Thr^{26} and MCa on RyR1 behavior. These evidences highlight the crucial role of this RyR1 region in the control of channel gating properties. MCa_b P-Thr^{26} will therefore represent an interesting tool to study the structural constraints that take place within the RyR1 MCa/MCa_b P-Thr^{26} binding site and that control RyR1 channel gating. A particular important question will be to understand how Thr^{26} of MCa interacts with RyR1 and what structural change is induced in RyR1 by the addition of a phosphate group or, more generally, a well-positioned negative charge on the lateral chain of the substituted residue at position 26 of MCa. Obviously, the recent resolution of the 3D structure of RyR1 (53–55) presents exciting perspectives on the understanding of the positive and negative allosteric modulation of this physiologically important ion channel. The data also need to be considered in the frame of an intriguing sequence homology between MCa and a cytoplasmic domain of the skeletal muscle voltage-gated calcium channel, the dihydropyridine receptor (DHPR) (9). Several studies have led to the proposal that MCa could mimic the action of this DHPR domain on RyR1 (56). Interestingly, this DHPR domain carries a Ser residue, Ser^{687}, corresponding to Thr^{26} of MCa, that has been previously shown to be phosphorylated in vitro by PKA (57, 58). In their study, the authors showed that a peptide corresponding to this sequence of DHPR completely loses its ability to activate RyR1 under phosphorylation of the Ser^{687} residue. Although DHPR II-III loop residues 681–690 do not seem essential for engaging physiological EC coupling in intact skeletal myotubes (59), our results suggest that MCa, and possibly the other calcin toxins with the inhibitor cystine knot motif, have evolved to mimic some aspect or aspects of interactions between the DHPR and RyR1, whose structures have been optimized for high affinity and efficacy toward functional modification of RyR1.

Both MCa P-Thr^{26} and MCa Thr^{26}Asp can now be considered interesting lead inhibitors of RyR1 channel activity. Both of these compounds freely cross the plasma membrane and can therefore be readily used to silence RyR1 channel activity in vitro. In vivo use can also be programmed because of the extreme protease resistance of MCa and important half-life in mice (24). Although MCa_b Thr^{26}Asp recapitulates some of the properties of MCa P-Thr^{26}, it does so only partially. Still better inhibitors may be designed that will not possess a phosphate group on the lateral chain. This is desirable if one wants to avoid dephosphorylation to occur in cellulo. Reasons why the aspartyl substitution only partially mimics the phosphate group on Thr^{26} may include an imperfect charge neutralization of Arg^{24}, the absence of a second negative charge that the phosphate group may carry depending on pH, and a less perfect interaction with RyR1 site. Obviously, several more analogs need to be designed to sort these issues out, but the basic observations are there that will help us design better inhibitors that are also phosphatase-resistant. The present compounds will nevertheless be useful to silence RyR1, and probably other RyR isoforms, in a number of pathological conditions in which abnormal RyR1 channel activity is involved. These include skeletal and cardiac myopathies (60), neurodegenerative disorders (61, 62), and environmentally triggered disorders (12). Our results suggest that MCa P-Thr^{26} is capable of normalizing two important dysfunctional properties of RyR1: by decreasing the sensitivity of RyR1 to cytoplasmic Ca^{2+}, allowing a decrease of spontaneous CICR (Fig. 3 *A–D*), and by normalizing RyR1 channel activity in the presence of high (50 μM) cytoplasmic Ca^{2+} (Fig. 3 *E* and *F*), restoring P_o to near those measured at $[Ca^{2+}]_{rest}$ (~120 nM). Coordinated reduction of abnormal RyR1opening mediated Ca^{2+} leak and normalization of RyR1 channel hyperactivity may have translational significance toward the development of new therapeutic strategies in treating the growing number of complex disorders that converge on RyR dysregulation.

In conclusion, these results represent the first demonstration, to our knowledge, that a small bioactive peptide toxin may undergo phosphorylation in cellulo at its site of delivery but also that such a modification has the ability to fully reprogram its pharmacological properties. Taking into account the growing list of active peptides isolated from venoms and the large spectra of posttranslational modifications, a systematic investigation of the effect of such toxin modification could lead to the characterization of new functionalities of these peptides. It is noteworthy that phosphorylated versions of bioactive peptides have also been detected in snake venoms (63), indicating that our observation may represent the first example, to our knowledge, of a larger list of peptides whose pharmacological activity is modulated by posttranslational modifications. Obviously, homologous peptides from the calcin family, which also bear the consensus phosphorylation site, are the next candidates for investigation of the effect of phosphorylation on pharmacology.

Materials and Methods

Detailed methods can be found in *SI Appendix, Materials and Methods*. Peptide syntheses were performed as previously described (7). The in cellulo phosphorylation was performed in HEK293 cells, using the PKA activator 8-bromoadenosine 3′,5′-cyclic monophosphate. NMR recordings were performed at a peptide concentration of 1 mM, using a Bruker DRX500 Avance III equipped with a QX1 probe. Junctional SR was from skeletal muscle of New Zealand White rabbits. [1H]-ryanodine binding and Ca^{2+} release experiments were performed at 0.1 mg/mL SR vesicles concentration. The interaction of MCa_b and MCa_b P-Thr^{26} with RyR1 was performed with purified RyR1. All planar bilayer experiments were performed using junctional SR membrane vesicles on a bilayer clamp BC 525C apparatus.

ACKNOWLEDGMENTS. We acknowledge the assistance of Mr. Jing Jie with some of the Ca^{2+} flux measurements made during revision of the manuscript. We thank Gamma Imaging Applications, Prométhée, and microscopie optique from Université Joseph Fourier for their collaboration. This work was supported by the French Agence Nationale de la Recherche (LabEx "Ion Channel Science and Therapeutics," Program ANR-11-LABX-0015), the Association Française contre les Myopathies, and the National Institutes of Health (Grants 1P01 AR52354, 2P01 ES011269, P42 ES004699, and US EPA STAR R829388 and R833292 to I.N.P. and W.F.).

1. Adams ME, Myers RA, Imperial JS, Olivera BM (1993) Toxityping rat brain calcium channels with omega-toxins from spider and cone snail venoms. *Biochemistry* 32(47): 12566–12570.
2. Adams ME, Olivera BM (1994) Neurotoxins: Overview of an emerging research technology. *Trends Neurosci* 17(4):151–155.
3. Calvete JJ (2013) Snake venomics: From the inventory of toxins to biology. *Toxicon* 75: 44–62.
4. King GF (2011) Venoms as a platform for human drugs: Translating toxins into therapeutics. *Expert Opin Biol Ther* 11(11):1469–1484.
5. Smith JJ, et al. (2011) Unique scorpion toxin with a putative ancestral fold provides insight into evolution of the inhibitor cystine knot motif. *Proc Natl Acad Sci USA* 108(26):10478–10483.
6. Zhu S, Darbon H, Dyason K, Verdonck F, Tytgat J (2003) Evolutionary origin of inhibitor cystine knot peptides. *FASEB J* 17(12):1765–1767.
7. Fajloun Z, et al. (2000) Chemical synthesis and characterization of maurocalcine, a scorpion toxin that activates Ca(2+) release channel/ryanodine receptors. *FEBS Lett* 469(2-3):179–185.
8. Chen L, et al. (2003) Maurocalcine and peptide A stabilize distinct subconductance states of ryanodine receptor type 1, revealing a proportional gating mechanism. *J Biol Chem* 278(18):16095–16106.
9. Estève E, et al. (2003) Critical amino acid residues determine the binding affinity and the Ca2+ release efficacy of maurocalcine in skeletal muscle cells. *J Biol Chem* 278(39): 37822–37831.
10. Imagawa T, Smith JS, Coronado R, Campbell KP (1987) Purified ryanodine receptor from skeletal muscle sarcoplasmic reticulum is the Ca2+-permeable pore of the calcium release channel. *J Biol Chem* 262(34):16636–16643.
11. Zimanyi I, Pessah IN (1991) Pharmacological characterization of the specific binding of [3H]ryanodine to rat brain microsomal membranes. *Brain Res* 561(2):181–191.
12. Pessah IN, Cherednichenko G, Lein PJ (2010) Minding the calcium store: Ryanodine receptor activation as a convergent mechanism of PCB toxicity. *Pharmacol Ther* 125(2):260–285.
13. Takeshima H, et al. (1994) Excitation-contraction uncoupling and muscular degeneration in mice lacking functional skeletal muscle ryanodine-receptor gene. *Nature* 369(6481):556–559.
14. Zimányi I, Buck E, Abramson JJ, Mack MM, Pessah IN (1992) Ryanodine induces persistent inactivation of the Ca2+ release channel from skeletal muscle sarcoplasmic reticulum. *Mol Pharmacol* 42(6):1049–1057.
15. Buck E, Zimanyi I, Abramson JJ, Pessah IN (1992) Ryanodine stabilizes multiple conformational states of the skeletal muscle calcium release channel. *J Biol Chem* 267(33): 23560–23567.
16. Fleischer S, Ogunbunmi EM, Dixon MC, Fleer EA (1985) Localization of Ca2+ release channels with ryanodine in junctional terminal cisternae of sarcoplasmic reticulum of fast skeletal muscle. *Proc Natl Acad Sci USA* 82(21):7256–7259.
17. Szappanos H, et al. (2005) Differential effects of maurocalcine on Ca2+ release events and depolarization-induced Ca2+ release in rat skeletal muscle. *J Physiol* 565(Pt 3): 843–853.
18. Lukács B, et al. (2008) Charged surface area of maurocalcine determines its interaction with the skeletal ryanodine receptor. *Biophys J* 95(7):3497–3509.
19. Altafaj X, et al. (2005) Maurocalcine and domain A of the II-III loop of the dihydropyridine receptor Cav 1.1 subunit share common binding sites on the skeletal ryanodine receptor. *J Biol Chem* 280(6):4013–4016.
20. Mabrouk K, et al. (2007) Critical amino acid residues of maurocalcine involved in pharmacology, lipid interaction and cell penetration. *Biochim Biophys Acta* 1768(10): 2528–2540.
21. Ram N, et al. (2008) Direct peptide interaction with surface glycosaminoglycans contributes to the cell penetration of maurocalcine. *J Biol Chem* 283(35): 24274–24284.
22. Poillot C, De Waard M (2011) [Potential of cell penetrating peptides for cell drug delivery]. *Med Sci (Paris)* 27(5):527–534.
23. Mosbah A, et al. (2000) A new fold in the scorpion toxin family, associated with an activity on a ryanodine-sensitive calcium channel. *Proteins* 40(3):436–442.
24. Tisseyre C, et al. (2014) Quantitative evaluation of the cell penetrating properties of an iodinated Tyr-L-maurocalcine analog. *Biochim Biophys Acta* 1843(10):2356–2364.
25. Tisseyre C, et al. (2013) Cell penetration properties of a highly efficient mini maurocalcine Peptide. *Pharmaceuticals (Basel)* 6(3):320–339.
26. Ram NT-NI, et al. (2011) In vitro and in vivo cell delivery of quantum dots by the cell penetrating peptide maurocalcine. *Int J Biomed Nanosci Nanotechnol* 2:12–32.
27. Stasiuk GJ, et al. (2011) Cell-permeable Ln(III) chelate-functionalized InP quantum dots as multimodal imaging agents. *ACS Nano* 5(10):8193–8201.
28. Zamaleeva AI, et al. (2014) Cell-penetrating nanobiosensors for pointillistic intracellular Ca2+-transient detection. *Nano Lett* 14(6):2994–3001.
29. Aroui S, Brahim S, De Waard M, Bréard J, Kenani A (2009) Efficient induction of apoptosis by doxorubicin coupled to cell-penetrating peptides compared to unconjugated doxorubicin in the human breast cancer cell line MDA-MB 231. *Cancer Lett* 285(1):28–38.
30. Aroui S, Brahim S, Waard MD, Kenani A (2010) Cytotoxicity, intracellular distribution and uptake of doxorubicin and doxorubicin coupled to cell-penetrating peptides in different cell lines: A comparative study. *Biochem Biophys Res Commun* 391(1): 419–425.
31. Aroui S, et al. (2009) Conjugation of doxorubicin to cell penetrating peptides sensitizes human breast MDA-MB 231 cancer cells to endogenous TRAIL-induced apoptosis. *Apoptosis* 14(11):1352–1365.
32. Aroui S, et al. (2009) Maurocalcine as a non toxic drug carrier overcomes doxorubicin resistance in the cancer cell line MDA-MB 231. *Pharm Res* 26(4):836–845.
33. Estève E, et al. (2005) Transduction of the scorpion toxin maurocalcine into cells. Evidence that the toxin crosses the plasma membrane. *J Biol Chem* 280(13): 12833–12839.
34. el-Hayek R, Lokuta AJ, Arévalo C, Valdivia HH (1995) Peptide probe of ryanodine receptor function. Imperatoxin A, a peptide from the venom of the scorpion Pandinus imperator, selectively activates skeletal-type ryanodine receptor isoforms. *J Biol Chem* 270(48):28696–28704.
35. Shahbazzadeh D, et al. (2007) Hemicalcin, a new toxin from the Iranian scorpion Hemiscorpius lepturus which is active on ryanodine-sensitive Ca2+ channels. *Biochem J* 404(1):89–96.
36. Schwartz EF, et al. (2009) Characterization of hadrucalcin, a peptide from Hadrurus gertschi scorpion venom with pharmacological activity on ryanodine receptors. *Br J Pharmacol* 157(3):392–403.
37. Poillot C, et al. (2010) D-Maurocalcine, a pharmacologically inert efficient cell-penetrating peptide analogue. *J Biol Chem* 285(44):34168–34180.
38. Marty I, Villaz M, Arlaud G, Bally I, Ronjat M (1994) Transmembrane orientation of the N-terminal and C-terminal ends of the ryanodine receptor in the sarcoplasmic reticulum of rabbit skeletal muscle. *Biochem J* 298(Pt 3):743–749.
39. Boisseau S, et al. (2006) Cell penetration properties of maurocalcine, a natural venom peptide active on the intracellular ryanodine receptor. *Biochim Biophys Acta* 1758(3): 308–319.
40. Endo M, Tanaka M, Ogawa Y (1970) Calcium induced release of calcium from the sarcoplasmic reticulum of skinned skeletal muscle fibres. *Nature* 228(5266):34–36.
41. Pessah IN, Zimanyi I (1991) Characterization of multiple [3H]ryanodine binding sites on the Ca2+ release channel of sarcoplasmic reticulum from skeletal and cardiac muscle: Evidence for a sequential mechanism in ryanodine action. *Mol Pharmacol* 39(5):679–689.
42. Ram N, et al. (2008) Design of a disulfide-less, pharmacologically inert, and chemically competent analog of maurocalcine for the efficient transport of impermeant compounds into cells. *J Biol Chem* 283(40):27048–27056.
43. Theillet FX, et al. (2013) Site-specific NMR mapping and time-resolved monitoring of serine and threonine phosphorylation in reconstituted kinase reactions and mammalian cell extracts. *Nat Protoc* 8(7):1416–1432.
44. Lowry DF, Ahmadian MR, Redfield AG, Sprinzl M (1992) NMR study of the phosphate-binding loops of Thermus thermophilus elongation factor Tu. *Biochemistry* 31(11): 2977–2982.
45. Woods AS, Ferré S (2005) Amazing stability of the arginine-phosphate electrostatic interaction. *J Proteome Res* 4(4):1397–1402.
46. Donald JE, Kulp DW, DeGrado WF (2011) Salt bridges: Geometrically specific, designable interactions. *Proteins* 79(3):898–915.
47. Sims RJ, 3rd, Reinberg D (2008) Is there a code embedded in proteins that is based on post-translational modifications? *Nat Rev Mol Cell Biol* 9(10):815–820.
48. Nishi H, Hashimoto K, Panchenko AR (2011) Phosphorylation in protein-protein binding: Effect on stability and function. *Structure* 19(12):1807–1815.
49. Buczek O, Bulaj G, Olivera BM (2005) Conotoxins and the posttranslational modification of secreted gene products. *Cell Mol Life Sci* 62(24):3067–3079.
50. Ferrer-Montiel AV, Canaves JM, DasGupta BR, Wilson MC, Montal M (1996) Tyrosine phosphorylation modulates the activity of clostridial neurotoxins. *J Biol Chem* 271(31):18322–18325.
51. Samsó M, Trujillo R, Gurrola GB, Valdivia HH, Wagenknecht T (1999) Three-dimensional location of the imperatoxin A binding site on the ryanodine receptor. *J Cell Biol* 146(2):493–499.
52. Zalk R, et al. (2015) Structure of a mammalian ryanodine receptor. *Nature* 517(7532): 44–49.
53. Yan Z, et al. (2015) Structure of the rabbit ryanodine receptor RyR1 at near-atomic resolution. *Nature* 517(7532):50–55.
54. Efremov RG, Leitner A, Aebersold R, Raunser S (2015) Architecture and conformational switch mechanism of the ryanodine receptor. *Nature* 517(7532):39–43.
55. Lau K, Van Petegem F (2014) Crystal structures of wild type and disease mutant forms of the ryanodine receptor SPRY2 domain. *Nat Commun* 5:5397.
56. Pouvreau S, et al. (2006) Transient loss of voltage control of Ca2+ release in the presence of maurocalcine in skeletal muscle. *Biophys J* 91(6):2206–2215.
57. Lu X, Xu L, Meissner G (1995) Phosphorylation of dihydropyridine receptor II-III loop peptide regulates skeletal muscle calcium release channel function. Evidence for an essential role of the beta-OH group of Ser687. *J Biol Chem* 270(31):18459–18464.
58. Imagawa T, Leung AT, Campbell KP (1987) Phosphorylation of the 1,4-dihydropyridine receptor of the voltage-dependent Ca2+ channel by an intrinsic protein kinase in isolated triads from rabbit skeletal muscle. *J Biol Chem* 262(17):8333–8339.
59. Proenza C, Wilkens CM, Beam KG (2000) Excitation-contraction coupling is not affected by scrambled sequence in residues 681-690 of the dihydropyridine receptor II-III loop. *J Biol Chem* 275(39):29935–29937.
60. Bers DM (2014) Cardiac sarcoplasmic reticulum calcium leak: Basis and roles in cardiac dysfunction. *Annu Rev Physiol* 76:107–127.
61. Del Prete D, Checler F, Chami M (2014) Ryanodine receptors: Physiological function and deregulation in Alzheimer disease. *Mol Neurodegener* 9:21.
62. Paula-Lima AC, Adasme T, Hidalgo C (2014) Contribution of Ca2+ release channels to hippocampal synaptic plasticity and spatial memory: Potential redox modulation. *Antioxid Redox Signal* 21(6):892–914.
63. Munawar A, et al. (2011) Venom peptide analysis of Vipera ammodytes meridionalis (Viperinae) and Bothrops jararacussu (Crotalinae) demonstrates subfamily-specificity of the peptidome in the family Viperidae. *Mol Biosyst* 7(12):3298–3307.